# Interference effects in IR photon echo spectroscopy of liquid water

Yeremenko, S; Pshenitchnikov, Maxim; Wiersma, DA; Pshenitchnikov, Maxim

*Published in:*
Physical Review A

*DOI:*
10.1103/PhysRevA.73.021804



*Publication date:*
2006

PHYSICAL REVIEW A **73**, 021804(R) (2006)

# Interference effects in IR photon echo spectroscopy of liquid water

Sergey Yeremenko, Maxim S. Pshenichnikov,* and Douwe A. Wiersma
*Ultrafast Laser and Spectroscopy Laboratory, Materials Science Centre, University of Groningen, Nijenborgh 4, 9747 AG Groningen, The Netherlands*
(Received 31 August 2005; published 22 February 2006)

Heterodyne-detected transient grating experiments on the OH-stretch mode of HDO dissolved in $D_2O$ resolve two distinctly different contributions originating from the initially excited OH stretch and the OD stretch which is thermally activated during the OH population relaxation. It is demonstrated that interference of both contributions greatly affects the outcome of IR photon echo experiments.

DOI: 10.1103/PhysRevA.73.021804 PACS number(s): 42.62.Fi, 42.65.An, 78.47.+p

Water, being a relatively simple substance in the form of a single, isolated molecule, possesses intricate and even peculiar properties in the liquid phase [1]. The complexity of liquid water is largely determined by a three-dimensional (3D) network of hydrogen bonds, which is in constant movement on ultrafast time scales. Recent years have witnessed an impressive progress in studying the dynamical processes in water due to considerable advances in IR femtosecond spectroscopy [2,3]. Especially different photon echo (PE) techniques have been proven exceptionally useful in unraveling the water dynamics at subpicosecond time scales [4–13]. These experimental and theoretical studies are mainly focused on the OH or OD stretching vibrations of an HDO molecule embedded in $D_2O$ or $H_2O$, respectively. In this manner, a number of unwanted complications such as excitation delocalization or Förster energy transfer [14] is circumvented. The normal or heavy water around the HDO molecule is deemed as a dynamical bath in a similar fashion as outlined by the Multimode Brownian Oscillator (MBO) model for electronic transitions [15] while the probe OH/OD stretching vibration is considered to be "the system." The bath modulates the vibrational frequency of the system and can in turn react to the state of the system (i.e., excited vibration) to account for the vibrational Stokes shift [16].

The OH/OD molecular stretching vibration is incredibly sensitive to the strength of the hydrogen bond network [3,17,18]. The picosecond stretching mode lifetime provides a fast and efficient energy transfer from the pump-excited OH/OD oscillators to low-frequency thermal modes raising temperature in the focal volume. As a result, the hydrogen-bond network weakens or even breaks [19] which changes the dynamical bath around the probe HDO molecule [20–22]. Consequently, the OH/OD stretch absorption of the probe HDO molecule decreases and its spectrum shifts toward higher frequencies [23]. The backreaction of the bath to the system has been successfully incorporated into the MBO model to account for a number of experimental features observed in pump-probe spectroscopy [5,11,19]. However, attempts to straightforwardly transfer this approach to the transient grating (TG) and PE echo spectroscopy required an unrealistically high temperature jump of $\sim 10$'s K [5,11] which is about a factor of 10 higher than could be supplied by excitation pulses. Therefore, there should exist another, more proficient factor than mere OH/OD absorption changes that influences the outcome of TG and PE experiments.

In this paper we demonstrate that the picosecond relaxation dynamics observed in IR, TG, and PE spectroscopy on diluted solution of HDO in $D_2O$, result mainly from temperature-induced modulation of the $D_2O$ refractive index. Heterodyning of the TG signal reveals two distinctly different contributions originating from the initially excited OH-stretch mode of the HDO molecule ("the system") and the initially unperturbed OD stretch of $D_2O$ ("the bath"). The latter is thermally excited during the OH population relaxation and forms a spatial grating of the $D_2O$ refractive index. As both contributions are intrinsically coherent, they interfere constructively or destructively depending on their phase relations.

Experimentally, the 70 fs, 10 $\mu$m IR output of the optical parametrical amplifier is split into four parts to obtain three excitation beams of approximately equal intensities with wave vectors $\mathbf{k}_1$, $\mathbf{k}_2$, and $\mathbf{k}_3$, and the local oscillator with an intensity reduced by three orders of magnitude (Fig. 1). The local oscillator beam is aligned collinearly with the echo signals at the $\mathbf{k}_4=\mathbf{k}_3+\mathbf{k}_2-\mathbf{k}_1$ direction to provide its heterodyning by scanning the time delay $t$. The sample, a 0.6 M solution of HDO molecules in $D_2O$ at room temperature, is pumped through a sapphire nozzle to form a 100-$\mu$m-thick freestanding.

Several representative interferograms in the TG configuration are shown in Fig. 2(a). At early waiting times $T$, the heterodyned TG signal is shifted to $t \approx 30$ fs and has a width of $\sim 180$ fs which is consistent with the near-resonant response of the OH stretch. However, at longer waiting times

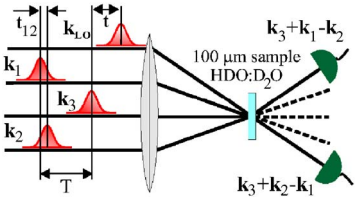


FIG. 1. (Color online) Schematic of the experimental arrangement.

*Electronic address: M.S.Pchenitchnikov@rug.nl

 

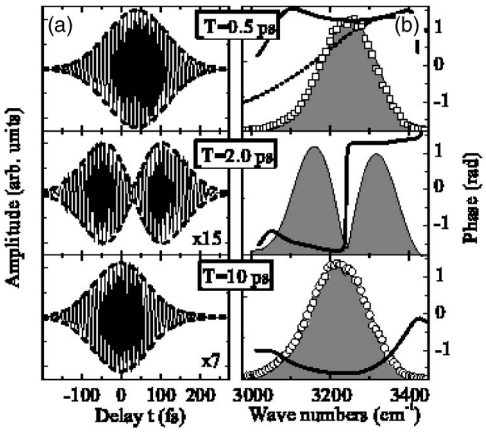


FIG. 2. Experimental heterodyned TG transients (a) and their Fourier-transforms (b) for waiting times $T=0.5$, 2, 10 ps. Dashed curves in (a) show the fit to the experimental data with the carrier frequency filtered out. The spectral amplitudes and phases in (b) are depicted as shaded contours and thick solid curves, respectively. Open squares and circles in (b) depict spectra of the OH-stretch response and IR pulses, respectively. The central frequency of the excitation pulses is detuned by $\sim 175$ cm$^{-1}$ to the red from the OH-stretch absorption maximum.

($T \approx 2$ ps) an additional component appears that interferes destructively with the resonant OH signal. The second contribution becomes dominant at $T=3 \div 4$ ps, and remains unchanged up to all experimentally accessible delays ($\sim 200$ ps). The heterodyned TG signal at long waiting times peaks at $t=0$ while its duration diminishes to $\sim 150$ fs, which corresponds to the width of the interferometric correlation function of the applied IR pulses.

As the interferograms contain both amplitudes and phases, we Fourier transform them to obtain the spectral contents of the time-resolved TG signals [Fig. 2(b)]. At the waiting time of $T=0.5$ ps the spectrum matches well the resonant TG spectrum (open squares) that is approximately equal to a product of the excitation pulse spectrum and the OH-stretch response. The latter was calculated as the amplitude of the complex linear susceptibility around both 0-1 and 1-2 vibrational transitions (dotted curve) which is a good approximation as most of the OH-stretch spectral dynamics have already completed by 0.5 ps [4,6,9,10,13]. The imaginary part of the susceptibility was obtained directly from a frequency-resolved, pump-probe experiment [22] while the real component was calculated via the Kramers-Kronig relations [24]. The central frequency of the excitation pulses was positioned close to the point where the emission and bleaching of the 0-1 transition is balanced by the induced absorption at the 1-2 transition ($\sim 3270$ cm$^{-1}$) thereby almost canceling the absorptive part of the susceptibility. Hence, the phase of the TG signal stays close to $+\pi/2$ [Fig. 2(b), solid curves]. In contrast to the earliest times, the TG spectrum at $T=10$ ps exactly matches the spectrum of excitation pulses (open circles). This, together with the zero-time shift of the heterodyned transient, points to the off-resonant origin of the TG response at long waiting times. In addition, the spectral phase of the signal undergoes a $\pi$ shift at long waiting times [Fig. 2(b)], which explains the destructive origin of the interference.

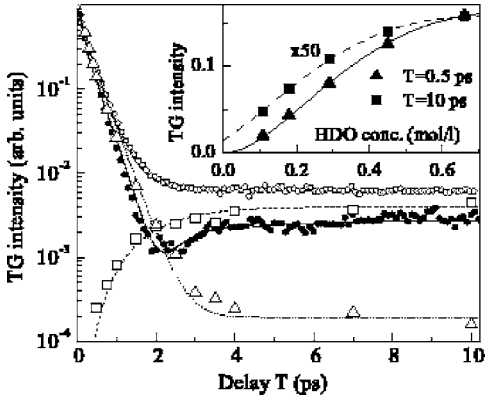


FIG. 3. Squared amplitudes of HDO (triangles) and $D_2O$ (squares) contributions to the TG signal for the 175 cm$^{-1}$ redshifted (solid dots) and 150 cm$^{-1}$ blueshifted (open circles) excitation spectrum. The inset shows the HDO concentration dependence of the TG signal at 0.5 ps (solid triangles) and 10 ps (solid squares). Curves are fits to the experimental data as explained in the text.

Therefore, the TG signal consists of two distinctly different contributions that are characterized by their own temporal amplitudes, frequencies, and phases. The contribution that dominates at short waiting times is clearly the near-resonant OH-stretch response. The second, off-resonant contribution, originates from a transition that is redshifted with respect to the IR pulse frequency as implied by the obtained phase of $-\pi/2$. The nearest resonance that meets this requirement is the OD stretch of heavy water (i.e., the bath) with a central wavelength of $\sim 2400$ cm$^{-1}$. However, this frequency is far beyond reach of the applied IR excitation pulses and thus there must be some indirect mechanism that leads to the bath excitation.

Figure 3 shows squared amplitudes of the two contributions obtained from the global fit of the experimental data (Fig. 2, dashed curves) along with the measured time-integrated (i.e., homodyne) TG signal. The near-resonant OH contribution (Fig. 3, triangles) decays monoexponentially by $\sim 4$ decimal orders before leveling off. Its doubled decay constant of 0.67 ps is in a good agreement with the $\sim 0.7$ ps [11,25] population lifetime of the OH-stretch of the HDO molecules dissolved in $D_2O$. The amplitude of the second contribution that has been previously attributed to the bath has a clearly delayed rise at a picosecond time scale and forms the constant background at large delays (Fig. 3, open squares). The sum of these contributions with their mutual phase taken in consideration excellently describes the experimental time-integrated TG signal (Fig. 3, thin curve).

To verify that the bath response is directly linked to the initial OH-stretch excitation, we performed a series of HDO concentration-dependent TG measurements (Fig. 3, inset). As we have already established, at the delay of $T=0.5$ ps (solid triangles) the signal mainly represents the OH-stretch response while at $T=10$ ps (solid squares) the response is chiefly from $D_2O$. The theoretical curves (solid lines) are calculated on the basis of pulse propagation in a strongly absorbing medium [24]. The apparent correlation between both dependencies confirms that the bath response is mainly induced by the OH-stretch excitation. However, a relatively

small portion of the signal (extrapolated to ~10%) appears even in neat $D_2O$, most probably, due to absorption of the combined resonances. This contribution plays a crucial role in the IR photon echo experiments (*vide infra*).

On the basis of the experimental data and their analysis, the following model of the bath response emerges: In the TG experiment the first pair of excitation pulses imprints in the sample a spatial grating of the OH-stretch population. The delayed probe pulse is diffracted off this grating to form the TG signal at the phase-matched direction. During the OH-stretch population relaxation, the stored vibrational energy is released into the bath forming a spatial grating of elevated temperatures. In turn, the temperature raise weakens and partially breaks the hydrogen-bond network [17,18] leading to changes in the shape and amplitude of the HDO- and $D_2O$-stretch transitions. The involvement of the former results in the leveling off of the TG contribution from the OH stretch at long delays (Fig. 3, triangles) in a similar fashion as was earlier observed in pump-probe experiments [19]. The $D_2O$ absorption grating is of little importance because there is a negligibly small overlap between the $D_2O$ absorption and pulse spectrum. In contrast, the spatial modulation of the $D_2O$ refractive index decreases with detuning from the resonant frequency only as the inverse detuning regardless of the particular absorption line shape [24]. Therefore, the probe pulse is scattered of the off-resonance grating written in the $D_2O$ refractive index (Fig. 3, open squares). This explains the fact that the phase of the heterodyned TG signal at long waiting times is almost $\pi$ shifted compared to the phase at short delays [Fig. 2(b)].

The outlined above scenario can be straightforwardly verified in the following way: if the frequency of the IR pulses is tuned to the blue side of the OH stretch, both OH-stretch and OD-stretch resonances become situated on the low frequency side of the laser pulse spectrum. The phase acquired from the OH-stretch transition changes its sign to amount to $\approx -\pi/3$ while the OD-induced phase remains unchanged. Therefore, the phase difference decreases from $\pi$ for the red-shifted laser to $\approx -\pi/3$, turning the destructive interference (i.e., $\cos\Delta\varphi \approx -1$) into a constructive one (i.e., $\cos\Delta\varphi \approx +1$) in a perfect agreement with the respective TG experiment (Fig. 3, open circles).

As can be seen from Fig. 3, the magnitude of the $D_2O$ contribution (open squares) at long delays exceeds by an order of magnitude the HDO contribution (open triangles) because the large frequency detuning from the $D_2O$ stretch is efficiently counterbalanced by a much higher (by a factor of 200) OD-bond concentration. The necessary temperature jump is estimated as 1–2 K which is in good agreement with the pump-probe measurement [22] as well as with an assessment made on the basis of known pulse energy, sample focal volume, and the water heat capacity. The analysis of the temporal dynamics of the OH and $D_2O$ contributions reveals another interesting feature of the relaxation process: the depopulation time of the OH stretch is noticeably shorter than the buildup time of the bath response. This hints that the OH-stretch relaxation occurs via an intermediate state or a manifold of such states [20,26–29].

The system-bath interference, observed in the TG experiment, is also inherently present in other three-pulse techniques, for instance, the stimulated photon echo. Figure 4 shows the results of the echo-peak shift (EPS) experiment. Here the delay $t_{12}$ between the first excitation pulses at which the integrated echo intensity is at maximum, is plotted as a function of the waiting time $T$. It has been shown [30–32] that the EPS closely mimics the key ingredient of the MBO model, the system-bath correlation function, providing a simple but powerful tool to study dynamical processes. For the redshifted excitation spectrum, the EPS function decreases rapidly at a time scale of ~0.5 ps, then rises again at ~2 ps, and finally falls off to ~1 fs (Fig. 4, triangles). For the blueshifted excitation spectrum the EPS function crosses zero at ~1 ps and stabilizes at negative values at ~2 ps (open diamonds). These features are qualitatively consistent with previous observations made with longer IR pulses [5].

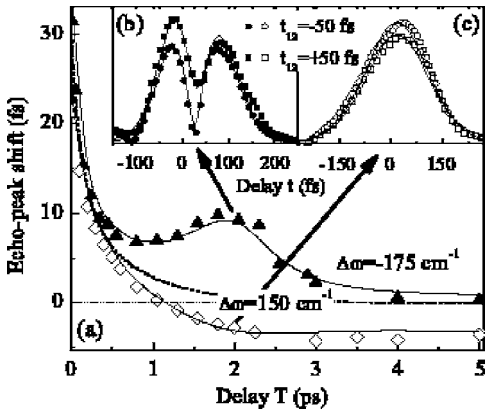


FIG. 4. EPS functions (a) and heterodyned transients at $T=2$ ps [(b) and (c)] in the case of the 175 cm$^{-1}$ redshifted (solid triangles) and 150 cm$^{-1}$ blue-shifted (open diamonds) pulse spectrum. Circles and squares show the experimental time-resolved (heterodyned) data for delay $t_{12}=50$ fs and $-50$ fs, respectively. The model correlation function is shown as a dashed curve. Solid curves are results of calculations as described in detail in Ref. [33].

The atypical EPS function behavior can be readily explained on the basis of the proposed model as arising from interference between the near-resonant OH-stretch and off-resonant $D_2O$ responses. The resonant signal that is governed by the OH-stretch excitation, has the $\omega_{OH}t_{12}$ phase dependence (where $\omega_{OH}$ is the OH-stretch frequency) while the phase of the nonresonant signal originating from direct $D_2O$ absorption, changes as $\omega_L t_{12}$, where $\omega_L$ is the laser frequency [15]. As a result, the phase difference obtained in the PE experiment, acquires an additional component $(\omega_L-\omega_{OH})t_{12}$ compared to its TG counterpart. Therefore, for the redshifted excitation, the phase difference decreases for positive delays $t_{12}$ making interference less destructive, while for negative delays $t_{12}$ destructive interference becomes more severe. This trend is clearly seen in Fig. 4(b), where the time-resolved transients for the delay $T=2$ ps are shown: the area beneath the $t_{12}=50$ fs transient is clearly larger than that in the case of $t_{12}=-50$ fs. The time-integrated signals that are measured in the EPS experiment, are proportional to the square of the area beneath time-resolved contours which explains the delayed raise of the EPS function. For the blue-shifted excitation spectrum, the situation is exactly opposite [Fig. 4(c)] leading to negative values of the EPS function [Fig. 4(a), diamonds].

The results of full-scale calculations according to the proposed scenario with the IR pulse electric fields and the system dynamics explicitly taken into consideration [33] are in good agreement with the experimental data (Figs. 3 and 4). Here we used a model biexponential system-bath correlation function,

$$\langle \delta\omega(t)\,\delta\omega(0)\rangle = \Delta_{fast}^2 \exp(-\Lambda_{fast}t) + \Delta_{slow}^2 \exp(-\Lambda_{slow}t) \tag{1}$$

with the following parameters: $1/\Lambda_{\mathrm{fast}} \cong 125$ fs, $\Delta_{\mathrm{fast}} \cong 90\ \mathrm{cm}^{-1}$, $1/\Lambda_{\mathrm{slow}} \cong 700$ fs, $\Delta_{\mathrm{slow}} \cong 65\ \mathrm{cm}^{-1}$ [33]. Despite its over simplicity at the short times [6,10,11,13,19], the long-time behavior is captured reasonably well which is the most relevant in these experiments. Note, that unlike the previous analysis [5], we do not require a nonzero value of the correlation function at the 2 ps delay because the transient signal asymmetry with the respect to the $t_{12}$ delay has interferometric (i.e., phase) rather than amplitude (i.e., photon-echo-like) origin. Therefore, no postulation of the tens of ps component in the correlation function is needed.

In conclusion, a series of heterodyne-detected TG and PE experiments on the OH-stretch vibration of HDO molecules dissolved in $D_2O$ have been performed. Heterodyning allowed us to separate different contributions to the TG signal and disentangle their respective amplitudes and phases. We directly demonstrated that the main part of the TG and PE signals at long decays originates from the spatial grating of the bath refractive index created by the OH-stretch vibration relaxation. This effect results from the high sensitivity of OD-stretch absorption spectra to the strength of the hydrogen-bond network that is weakened by the subsequent thermalization of the OH-stretch relaxation. At intermediate waiting times, the OH and $D_2O$ responses interfere either constructively or destructively which leads to a number of peculiar features in TG and PE measurements. Understanding of such interference phenomena is crucial for the accurate analysis of nonlinear ir spectroscopic experiments not only on water and its isotopic mixtures but also in other situations when the energy deposited to study the system affects the properties under investigation.

We thank the Nederlandse Stichting voor Fundamenteel Onderzoek der Materie (FOM) and the Materials Science Centre (MSC) of the University of Groningen for financial support. We are also indebted to H. Bakker for numerous fruitful discussions.

[1] F. Franks, in *Water: A Comprehensive Treatise* (Plenum, New York, 1972).
[2] E. T. J. Nibbering and T. Elsaesser, Chem. Rev. (Washington, D.C.) **104**, 1887 (2004).
[3] R. Rey, K. B. Moller, and J. T. Hynes, Chem. Rev. (Washington, D.C.) **104**, 1915 (2004).
[4] J. Stenger, D. Madsen, P. Hamm, E. T. J. Nibbering, and T. Elsaesser, Phys. Rev. Lett. **87**, 027401 (2001).
[5] J. Stenger *et al.*, J. Phys. Chem. A **106**, 2341 (2002).
[6] C. J. Fecko *et al.*, Science **301**, 1698 (2003).
[7] A. Piryatinski, C. P. Lawrence, and J. L. Skinner, J. Chem. Phys. **118**, 9672 (2003).
[8] A. Piryatinski, C. P. Lawrence, and J. L. Skinner, J. Chem. Phys. **118**, 9664 (2003).
[9] S. Yeremenko, M. S. Pshenichnikov, and D. A. Wiersma, Chem. Phys. Lett. **369**, 107 (2003).
[10] J. B. Asbury *et al.*, J. Phys. Chem. A **108**, 1107 (2004).
[11] C. J. Fecko *et al.*, J. Chem. Phys. **122**, 054506 (2005).
[12] M. L. Cowan *et al.*, Nature (London) **434**, 199 (2005).
[13] J. B. Asbury *et al.*, J. Chem. Phys. **121**, 12431 (2004).
[14] S. Woutersen and H. J. Bakker, Nature (London) **402**, 507 (1999).
[15] S. Mukamel, *Principles of Nonlinear Optical Spectroscopy* (Oxford University Press, New York, 1995).
[16] S. Woutersen and H. J. Bakker, Phys. Rev. Lett. **83**, 2077 (1999).
[17] G. E. Walrafen *et al.*, J. Chem. Phys. **85**, 6970 (1986).
[18] T. Iwata *et al.*, Appl. Spectrosc. **51**, 1269 (1997).
[19] T. Steinel *et al.*, J. Phys. Chem. A **108**, 10957 (2004).
[20] H.-K. Nienhuys *et al.*, J. Chem. Phys. **111**, 1491 (1999).
[21] A. J. Lock, S. Woutersen, and H. J. Bakker, J. Phys. Chem. A **105**, 1238 (2001).
[22] D. Cringus *et al.*, J. Phys. Chem. B **108**, 10376 (2004).
[23] F. O. Libnau *et al.*, J. Am. Chem. Soc. **116**, 8311 (1994).
[24] Y. R. Shen, *The Principles of Nonlinear Optics* (Wiley, New York, 1984).
[25] S. Woutersen, U. Emmerichs, H. K. Nienhuys, and H. J. Bakker, Phys. Rev. Lett. **81**, 1106 (1998).
[26] D. Cringus *et al.*, Chem. Phys. Lett. **408**, 162 (2005).
[27] A. M. Dokter, S. Woutersen, and H. J. Bakker, Phys. Rev. Lett. **94**, 178301 (2005).
[28] A. J. Lock and H. J. Bakker, J. Chem. Phys. **117**, 1708 (2002).
[29] J. C. Deak *et al.*, J. Phys. Chem. A **104**, 4866 (2000).
[30] W. P. de Boeij, M. S. Pshenichnikov, and D. A. Wiersma, Chem. Phys. Lett. **253**, 53 (1996).
[31] W. P. de Boeij, M. S. Pshenichnikov, and D. A. Wiersma, J. Chem. Phys. **100**, 11806 (1996).
[32] T. Joo *et al.*, J. Chem. Phys. **104**, 6089 (1996).
[33] S. Yeremenko, Ph.D. thesis, University of Groningen, 2004.